Table 3
Summary of cases of tumor seeding

No.	Age	Sex	Size (mm)	Location	Distance from pleura (mm)	Co-axial method	No. of biopsy	Technique of biopsy	Size of the needle
1	72	M	30	Right upper	0	No	1	Core biopsy	18G
2	73	M	30	Left lower	30	Yes	3	Core biopsy	18G
3	71	M	10	Right upper	20	No	2	Aspiration biopsy	22G
4	30	F	28	Left upper	76	No	2	Core biopsy	18G
5	69	M	15	Right lower	0	No	2	Core biopsy	21G
6	77	M	12	Right upper	30	Yes	2	Core biopsy	20G

rate of 0.06%, which also shows no major difference from the previously reported complication rate. However, in the present study, there were several cases of severe complications including cardiac and respiratory arrest, and shock, which can be secondary to air embolism, although it is very difficult to confirm air embolism in the coronary artery in cases of myocardial infarction when the patient has not been scanned at the level of the heart. It is speculated that concurrent cough during the procedure has a high possibility of an air embolism misplacing the biopsy needle into the large vessel adjacent to the pulmonary lesion. Among the total of six cases with air emboli in the present study, two cases demonstrated biopsied pulmonary lesions located close to the large vessels, however the remaining four cases have no close relation to the large vessels. There were no reports of coughing during the procedure in any of the cases complicated by air embolism. Air embolism even occurred in a case in which the nodule was very near the pleura (case no. 5). In our study, all cases with air emboli had undergone CT-guided biopsy using a core biopsy needle of 18–20 gauge, which is greater in diameter than the usually used fine aspiration needles. Having said that, in the previous reviews, most cases with air emboli were biopsied by fine aspiration needles, and there are two prior reports of air embolism following CT-guided lung needle marking using thin needles without recent biopsy [24–26].

Tumor seeding into the needle tract seems to be a rare possibility in several case reports [27–34]. There were six cases (0.06%) of tumor seeding in our study, which is a relatively high frequency compared to previous studies [5,35]. The true incidence of tumor seeding along the needle may be underestimated as not all cases can be diagnosed, and many patients die before these metastases become clinically apparent. Tumor seeding appears to depend on the size of the needle, therefore large-bore needles carry a relatively greater risk of tumor seeding, however tumor seeding following a fine needle aspiration was reported in one case of our study. It is thought that CT-guided biopsy performed using the Co-axial method has less frequency of tumor seeding as the outer cannula minimizes direct contact of the tumor cells with the biopsy route. Surprisingly, tumor seeding occurred in two cases using the Co-axial method. We speculate that the outer cannula was not appropriately placed.

Unfortunately, there were seven patients (0.07%) who died in our study due to complications in the CT-guided needle biopsy. Greene [6] estimated the mortality rate associated with fine needle aspiration to be 0.02%, how-

ever Richardson et al. [8] reported eight deaths (0.15%) in their study due to complications in CT-guided needle biopsy. Most of the deaths in the present study were attributed to fatal air embolism. Three cases of air embolism that were treated with hyperbaric oxygen recompression were recovered without sequela, which may suggest hyperbaric oxygen recompression therapy is effective for treatment of air embolism, and for reducing the mortality rate.

Our study has several limitations, including selection bias, the long period of the study, multi-center analysis with a large variety of techniques and CT scanners, and the possibility of missing or misdiagnosing significant complications such as the number of air emboli and tumor seeding. Moreover, our study is a retrospective questionnaire-based analysis rather than a prospective survey.

In conclusion, this is the first nation-wide study documenting severe complications with respect to CT-guided needle biopsy in Japan. The complication rate in Japan is comparable to internationally published figures. We believe this data will improve both clinicians as well as patients understanding of the risk versus benefit of CT-guided needle biopsy, resulting better decisions.

Acknowledgement

References

[1] Sinner WN. Pulmonary neoplasms diagnosed with transthoracic needle biopsy. Cancer 1979;43:1533–40.

[2] Klein JS, Zarka MA. Transthoracic needle biopsy. J Thorac Imag 1997;12:232–49.

[3] Hirose T, Mori K, Machida S, et al. Computed tomographic fluoroscopy-guided transthoracic needle biopsy for diagnosis of pulmonary nodules. Jpn J Clin Oncol 2000;30:259–62.

[4] Berquist TH, Bailey PB, Cortese DA, et al. Transthoracic needle biopsy: accuracy and complication in relation to location and type of lesion. Mayo Clin Proc 1980;55:475–81.

[5] Sinner WN. Complications of percutaneous transthoracic needle aspiration biopsy. Acta Radiol Diag 1976;17:813–28.

[6] Greene RE. Transthoracic needle aspiration biopsy. In: Athanasoulis CA, Pfister RC, Greene RE, Robertson GH, editors. Interventional radiology. Philadelphia: Sanders; 1982. p. 587–634.

[7] Klein JS, Zarka MA. Transthoracic needle biopsy. Radiol Clin North Am 2000;38:235–66.

[8] Richardson CM, Pointon KS, Manhire AR, et al. Percutaneous lung biopsies: a survey of UK practice based on 5444 biopsies. Br J Radiol 2002;75:731–5.

[9] Belfiore G, Filippo SD, Guida C, et al. CT-guided needle biopsy of lesions. Nucle Med Biol 1994;21:713–9.

[10] Wescott JL. Air embolism complicating percutaneous needle biopsy of the lung. Chest 1973;63. pp. 108–108.

[11] Aberle DR, Gamsu G, Golden JA. Fatal systemic arterial air embolism following lung needle aspiration. Radiology 1987;165:351–3.

[12] Cianci P, Posin JP, Shimshak RR, et al. Air embolism complicating percutaneous thin needle biopsy of lung. Chest 1987;92:749–50.

[13] Tolly TL, Feldmeier JE, Czarnecki D. Air embolism complicating percutaneous lung biopsy. AJR Am J Roentgenol 1988;150:555–6.

[14] Baker BK, Awwad EE. Computed tomography of fatal cerebral air embolism following percutaneous aspiration biopsy of the lung. JCAT 1988;12:1082–3.

[15] Worth ER, Burton RJ, Landreneau RJ, Eggers GWN, et al. Left atrial air embolism during intraoperative needle biopsy of a deep pulmonary lesion. Anesthesiology 1990;73:342–5.

[16] Wong RS, Ketai L, Temes RT, Follis FM, et al. Air embolus complicating transthoracic percutaneous needle biopsy. Ann Thorac Surg 1995;59:1010–1.

[17] Khatri S. Cerebral artery gas embolism (CAGE) following fine needle aspiration biopsy of the lung. Aust NZ J Med 1997;27. pp. 27–27.

[18] Regge D, Gallo T, Galli J, et al. Systemic arterial air embolism and tension pneumothorax: two complications of transthoracic percutaneous thin-needle biopsy in the same patient. Eur Radiol 1997;7:173–5.

[19] Kodama F, Ogawa T, Hashimoto M, et al. Fatal air embolism as a complication of CT-guided needle biopsy of the lung. JCAT 1999;23:949–51.

[20] Shetty PG, Fatterpekar GM, Manohar S, et al. Fat cerebral air embolism as a complication of transbronchoscopic lung biopsy: a case report. Aust Radiol 2001;45:215–7.

[21] Arnold BW, Zwiebel WJ. Percutaneous transthoracic needle biopsy complicated by air embolism. AJR Am J Roentgenol 2002;178:1400–2.

[22] Mokhlesi B, Ansaarie I, Bazen B, et al. Coronary artery air embolism complicating a CT-guided transthoracic needle biopsy of the lung. Chest 2002;121:993–6.

[23] Laurent F, Montaudon M, Latrabe V, et al. Percutaneous biopsy in lung cancer. Eur J Radiol 2003;45:60–8.

[24] Ohi S, Ito Y, Keiya H, et al. Air embolism following computed tomography-guided lung needle marking; report of a case. Kyobu-Geka 2004;57:421–3.

[25] Kamiyoshihara M, Sakata K, Ishikawa S, et al. Cerebral arterial air embolism following CT-guided lung needle marking; report of a case. J Cardiovasc Surg 2001;42:699–700.

[26] Sakiyama S, Kondo K, Matsuoka H, et al. Fatal air embolism during computed tomography-guided pulmonary marking with a hook-type maker. J Thorac Cardiovasc Surg 2003;126:1207–9.

[27] Muller NL, Bergin CJ, Miller RR, et al. Seeding of malignant cells into the needle track after lung and pleural biopsy. J Can Assoc Radiol 1986;37:192–4.

[28] Redwood N, Beggs D, Morgan WE. Dissemination of tumor cells from fine needle biopsy. Thorax 1989;44:826–7.

[29] Berger RL, Dargan EL, Huang BL, et al. Dissemination of cancer cells by needle biopsy of the lung. J Thor Cardiovasc Surg 1972;63:430–2.

[30] Freise G, Larios R, Takeno Y, et al. Cell dissemination and implantation of neoplasms through biopsy and excision of malignant tumors. Dis Chest 1967;52:485–9.

[31] Christensen ES. Iatrogenic dissemination of tumor cells. Dissemination of tumour cells along the needle track after percutaneous, transthoracic lung biopsy. Danish Med Bull 1978;25:82–7.

[32] Ferrucci JT, Wittenberg J, Margolies MN, et al. Malignant seeding of the tract after thin-needle aspiration biopsy. Radiology 1979;130:345–6.

[33] Yoshikawa T, Yoshida J, Nishimura M, et al. Lung cancer implantation in the chest wall following percutaneous fine needle aspiration biopsy. Jpn J Clin Oncol 2000;30:450–2.

[34] Kara M, Alver G, Sak SD, Kavukcu S. Implantation metastasis caused by fine needle aspiration biopsy following curative resection of stage IB non-small cell lung cancer. Eur J Cardiothor Surg 2001;20:868–70.

[35] Ayar D, Golla B, Lee JY, Nath H. Needle-track metastasis after transthoracic needle biopsy. J Thorac Imag 1998;13:2–6.

Detection of *EGFR* Mutations in Archived Cytologic Specimens of Non-Small Cell Lung Cancer Using High-Resolution Melting Analysis

Kiyoaki Nomoto, CT,[1] Koji Tsuta, MD,[1] Toshimi Takano, MD,[2] Tomoya Fukui, MD,[2] Karin Yokozawa,[3] Hiromi Sakamoto, MD,[4] Teruhiko Yoshida, MD,[4] Akiko Miyagi Maeshima, MD,[5] Tatsuhiro Shibata, MD,[5] Koh Furuta, MD,[3] Yuichiro Ohe, MD,[2] and Yoshihiro Matsuno, MD[1]

Abstract

Mutations of the epidermal growth factor receptor (EGFR), particularly deletional mutations (DEL) in exon 19 and L858R in exon 21, are reportedly correlated with clinical outcome in patients with non–small cell lung cancer (NSCLC) receiving the EGFR tyrosine kinase inhibitors gefitinib and erlotinib, suggesting that detection of EGFR mutations would have an important role in clinical decision making. We established and validated an easy, inexpensive, and rapid method for detecting DEL and L858R from cytologic material by high-resolution melting analysis (HRMA). Dilution for sensitivity studies revealed that DEL and L858R were detectable in the presence of at least 10% and 0.1% EGFR-mutant cells, respectively. We analyzed 37 archived cytological slides of specimens from 29 patients with advanced NSCLC and compared the results with direct sequencing data obtained previously. Of 37 samples, 34 (92%) yielded consistent results with direct sequencing, 2 were false negative, and 1 was indeterminate. The sensitivity of this analysis was 90% (19/21) and specificity, 100% (15/15). These results suggest that HRMA of archived cytologic specimens of advanced NSCLC is useful for detecting EGFR mutations in clinical practice.

Increased expression of epidermal growth factor receptor (EGFR) has been reported in carcinomas of various organs, including of the lung, and has been shown to have a crucial role in tumor progression.[1,2] Gefitinib (Iressa, AstraZeneca, Osaka, Japan) is an orally active, selective EGFR tyrosine kinase inhibitor that binds to the adenosine triphosphate binding pocket of the kinase domain and blocks downstream signaling pathways. Clinical phase 2 studies have demonstrated gefitinib antitumor activity in patients with advanced non–small cell lung cancer (NSCLC).[3,4] Although some of these studies have shown that the rate of response to gefitinib is higher in women, patients with adenocarcinoma, patients who have never smoked, and Japanese and East Asians,[3-5] no predictive molecular marker had been discovered until April 2004, when somatic mutations in the kinase domain of *EGFR* were suggested to be correlated with gefitinib sensitivity.[6,7] Thereafter, several studies revealed a strong association between *EGFR* mutations and clinical outcome in parameters such as response rate, time to progression, and overall survival in consecutive NSCLC patients treated with gefitinib.[8-10]

Many types of *EGFR* mutation have been identified.[6-16] They are concentrated in exons 18 to 21 of *EGFR*, close to the region encoding the adenosine triphosphate binding pocket, and about 90% of patients with *EGFR* mutations have mutations in 2 hotspots: in-frame deletions including amino acids at codons 747 to 749 (DEL) in exon 19 and a missense mutation at codon 858 (L858R) in exon 21.

The mutational status of *EGFR*, especially DEL and L858R, is a strong predictor of gefitinib sensitivity, and detection of such mutations would provide patients and physicians with important information for optimal choice of therapy. Therefore, analysis of a sufficient number of tumor samples in

good condition and direct sequencing after laser capture microdissection (LCM) is considered the "gold standard" for detecting *EGFR* mutations. However, this approach is not necessarily practical for clinical use for a number of reasons. First, tumor samples with a large volume and in good condition are difficult to obtain in most cases of advanced NSCLC. Second, LCM and direct sequencing require special instruments and are time-consuming and costly. Therefore, it is necessary to establish practical and precise methods for detecting *EGFR* mutations from easily obtainable diagnostic samples, which usually contain a small number of tumor cells and a large number of normal cells.

The real-time reverse transcription–polymerase chain reaction (PCR) assay has been reported for detection of *EGFR* mutations.[17] In this method, many samples can be genotyped within a few hours without the need for post-PCR sample manipulation, although expensive fluorescence-labeled probes and restriction enzymes are needed. A new inexpensive dye, SYBR Green I, has been developed,[18] but this limits the melting resolution because of dye redistribution during melting.

Recently, studies have validated the usefulness of high-resolution melting analysis (HRMA) using LCGreen I dye for mutational analysis,[19-22] and another study has validated analysis using cytologic samples for c-kit.[23] The advantages of this approach are that labeling of either primer with dye is not needed and PCR amplification and melting analysis can be performed in the same capillary tube, minimizing sample handling and reducing the possibility of error and sample contamination. HRMA is easy, rapid, and inexpensive to perform and has considerable potential for mutation detection in clinical practice.

We report a new method for detecting DEL and L858R from archival Papanicolaou-stained cytologic slides by HRMA. We validated the method by comparing the results with direct sequencing data from specimens surgically resected from the same patients. We also performed a titration assay to evaluate the lower limit of the proportion of tumor cells for detection of *EGFR* mutations by using a mixture of wild-type (WT) and *EGFR*-mutant lung cancer cell lines.

Materials and Methods

Cell Lines and Titration Assay

We performed dilution for sensitivity studies using 3 lung adenocarcinoma cell lines, NCI-H1650, NCI-H1975, and NCI-A549, obtained from the American Tissue Cell Collection (Manassas, VA). The H1650 cell line contains a DEL mutation (delE746-A750), the H1975 cell line contains the L858R mutation,[24] and the A549 cell line contains WT *EGFR*.[25] *EGFR* copy numbers in the H1650, H1975, and A549 cells are reported to be 2, 3, and 2.48 per cell, respectively.[25,26]

Dilutions of the *EGFR*-mutant cells (H1650 or H1975) with A549 cells were prepared using proportions of *EGFR*-mutant cells of 100% (no A549 cells), 10%, 1%, 0.1%, and 0% (no mutant cells). DNA extracted from each dilution was subjected to subsequent PCR assay.

DNA Extraction From Archived Cytologic Slides

With approval of the National Cancer Center Institutional Review Board, Tokyo, Japan, we performed *EGFR* gene analysis. Among the 66 cases analyzed in a previous study, diagnostic Papanicolaou-stained cytologic samples were available for 29. Of the patients, 5 had multiple (2 to 4) metachronous samples, and the total number of available cytologic samples was 37. Two clinical cytologists (K.N. and K.T.), who were unaware of the patients' characteristics and mutational status, examined these 37 samples. Cytologic parameters described for each slide included sampling procedure, approximate number of nucleated cells on each slide (<100, 100-499, 500-999, ≥1,000), and proportion of tumor cells among total nucleated cells (<10%, 10%-49%, 50%-89%, ≥90%). After this assessment, DNA was extracted from the cells on the slides using a QIAamp DNA Micro Kit (catalog No. 56304, QIAGEN, Valencia, CA) as follows: Coverslips were removed by immersion in xylene for 72 hours, and the slides were rinsed in 95% ethanol 3 times. Cells on the slides were removed by using sterilized disposable knives and suspended in ATL buffer containing Proteinase K in 1.5-mL tubes. Further procedures were performed according to the manufacturer's protocol.

In 2 samples with a small proportion of tumor cells, tumor cell–rich parts on the slides were marked with a diamond pen and selectively retrieved manually with a knife to enrich the proportion of tumor cells.

Polymerase Chain Reaction

Primer A was designed to amplify a region containing nucleotides 2235 to 2277 (amino acids E746 to I759) of *EGFR*, in which almost all reported deletional mutations in exon 19 occur.[6-16] The sequences of primer A were AAAATTCC-CGTCGCTATC (forward) and AAGCAGAAACTCACATCG (reverse). Primer B was designed to amplify a region containing nucleotides 2573 and 2582, at which point mutations L858R and L861Q in exon 21 occur, respectively. L858R and L861Q account for about 96% and 2%, respectively, of all reported point mutations in exon 21.[6-16] The sequences of primer B were AGATCACAGATTTTGGGC (forward) and ATTCTTTCTCTTCCGCAC (reverse).

PCR was performed using these primers, Fast Start *Taq* Polymerase (Roche Diagnostics, Indianapolis, IN), and LCGreen I Gene Scanning Reagents (Idaho Technology, Salt Lake City, UT) on a LightCycler (Roche Diagnostics). The samples were denatured at 95°C for 10 minutes and then subjected

to 37 cycles of denaturing for 10 seconds at 95°C, annealing for 10 seconds at 60°C, and extension for 5 seconds at 72°C with primer A and 45 cycles of denaturing for 10 seconds at 95°C, annealing for 5 seconds at 56°C, and extension for 5 seconds at 72°C with primer B.

High-Resolution Melting Analysis

The PCR products were denatured at 95°C for 5 minutes and cooled to 40°C in the LightCycler to form heteroduplexes. The LightCycler capillary was transferred to an HR-1 (Idaho Technology), an HRMA instrument, and heated at a transition rate of 0.3°C per second. Data were acquired and analyzed using the accompanying software (Idaho Technology). After normalization and temperature-adjustment steps, melting curve shapes from 78.5°C to 85.5°C were compared between samples and control samples. Human Genomic DNA (Roche Diagnostics) was used as a control sample with wild-type *EGFR*.

Direct Sequencing .

In a previous study, we performed direct sequencing of *EGFR* in 66 cases of NSCLC that relapsed after primary surgery. Methanol-fixed, paraffin-embedded surgical specimens of primary NSCLC were obtained, and DNA was extracted from laser capture microdissected tumor tissue. Nested PCR was performed to amplify exons 18 to 24 of *EGFR* using

primers described previously.[8] Direct sequencing of the PCR products was performed using the ABI PRISM 3700 and 3100 DNA sequencers (Applied Biosystems, Foster City, CA).

Results

In the melting analysis using primer A (exon 19), 100% H1650 cells (EGFR DEL) gave a skewed curve from 100% A549 cells (EGFR WT). Mixtures of both cells gave gradual curves, and DEL could be detected in the presence of 10% but not 1% H1650 cells ∎Figure 1A∎. In the analysis using primer B (exon 21), 100% H1975 cells (EGFR L858R) gave a left-shifted curve from 100% A549 cells. Mixtures of both cells gave gradual curves, and L858R could be detected in the presence of 0.1% H1975 cells ∎Figure 1B∎.

We analyzed 37 archival cytologic samples from 29 patients by HRMA, and the results are summarized in ∎Table 1∎, in comparison with the results obtained by direct sequencing from surgically resected specimens of each patient. Eleven samples were obtained by bronchial brushing or washing, 4 by transbronchial fine-needle aspiration (FNA), 4 by percutaneous FNA of lung tumors, 2 by FNA of superficial lymph nodes, 14 from pleural effusion, and 2 from pericardial effusion. The median time between sampling and analysis was 3 years (range, 1-8 years).
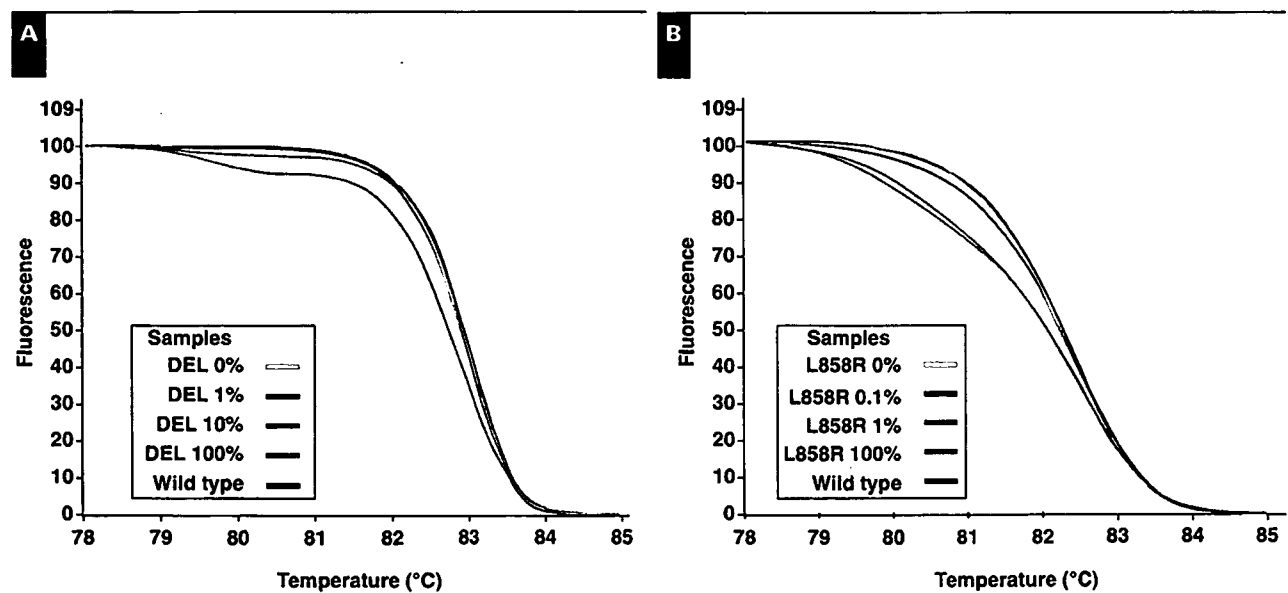
∎Figure 1∎ Adjusted melting curves obtained by high-resolution melting analysis of lung adenocarcinoma cells with primers designed to detect mutations in epidermal growth factor receptor (*EGFR*) exon 19 (**A**) or exon 21 (**B**). **A**, Mixtures of H1650 cells (*EGFR*ᴰᴱᴸ) and A549 cells (*EGFR*ᵂᵀ) revealed gradual curves; 100% and 10% H1650 cells were identified as containing a DEL mutation, and 1% H1650 cells were identified as wild type. **B**, Mixtures of H1975 cells (*EGFR*ᴸ⁸⁵⁸ᴿ) and A549 cells (*EGFR*ᵂᵀ) revealed gradual curves, and 100% to 0.1% H1975 cells were identified as containing the L858R mutation. DEL, deletional.

460

In the analysis of exon 19, thorough melting curves were obtained in 35 samples, whereas the other 2 samples (5 and 21) could not be analyzed because PCR was not complete in these cases. Among the 35 samples, 12 gave curves that were different from a WT obtained for cell line A549, as shown in ❚Figure 2A❚, and 23 samples revealed almost the same curves with a WT ❚Figure 2C❚ (Figure 2A). Because the skewed curves for the 12 samples were analogous to the curve for H1650 cells, we judged that they had DEL. In the analysis of exon 21, 7 and 2 samples gave left- and right-shifted curves from a WT, respectively, and 28 samples gave almost identical curves with a WT ❚Figure 2B❚ and ❚Figure 2D❚. Because the left-shifted curves of the 7 samples were analogous to the curve for H1975, we judged that they had L858R.

As mentioned previously, 2 samples (21 and 25) showing right-shifted curves were considered inadequate for evaluation because of incomplete PCR (Figures 2C and 2D). Taken together, DEL was detected in 12 samples (8 patients) and L858R was detected in 7 samples (6 patients) among 37 samples (29 patients). Samples 5 and 25 were insufficient for judging genotypes of 1 hotspot but judged as containing mutations in the other hotspot (L858R and DEL, respectively). Therefore, the genotype was indeterminate in only 1 sample (case 21) and determined as WT in 17 samples (14 patients). Analysis of the 5 cases with multiple (2 to 4) metachronous samples revealed no differences of genotype in each case.

The results of HRMA were consistent with those of direct sequencing in all samples except samples 19 and 20 (Table 1), which revealed WT curves by HRMA, although

❚Table 1❚
HRMA Results for 37 Archival Cytologic Samples From 29 Patients

Sample No.	Histologic Type	Sampling Method	No. of Nucleated Cells	Proportion of Cancer Cells/Nucleated Cells (%)	Mutational Analysis by HRMA		Mutational Analysis by Direct Sequencing
					DEL	L858R	
1	Ad	TBAC	≥1,000	≥90	WT	L858R	L858R
2	Ad	PAC	500-999	≥90	WT	L858R	L858R
3	Ad	BC	500-999	≥90	WT	L858R	L858R
4	Ad	BC	500-999	10-49	DEL	WT	delL747-E749
5	Ad	BC	500-999	50-89	NE	L858R	L858R
6	Ad	BC	≥1,000	<10	WT	WT	WT
7	Ad	BC	100-499	≥90	WT	WT	WT
8	Ad	LN	≥1,000	50-89	WT	WT	WT
9a	Ad	BC	500-999	50-89	WT	WT	WT
9b		BC	500-999	≥90	WT	WT	WT
9c		BC	100-499	<10	WT	WT	WT
10	Ad	PL	≥1,000	10-49	DEL	WT	delE746-A750
11a	Ad	PL	≥1,000	≥90	WT	L858R	L858R
11b		PL	500-999	50-89	WT	L858R	L858R
12	Ad	PL	≥1,000	<10	WT	WT	WT
13	SCC	PAC	500-999	50-89	WT	WT	WT
14a	Ad	PC	≥1,000	50-89	DEL	WT	delE746-A750
14b		PL	500-999	50-89	DEL	WT	delE746-A750
14c		PL	≥1,000	50-89	DEL	WT	delE746-A750
14d		PL	500-999	10-49	DEL	WT	delE746-A750
15a	Pleo	BC	100-499	50-89	DEL	WT	delE746-A750
15b		BC	500-999	50-89	DEL	WT	delE746-A750
16	Ad	PAC	100-499	10-49	WT	WT	WT
17	Ad	PL	500-999	50-89	WT	L858R	L858R/E709K
18	Ad	TBAC	500-999	≥90	WT	WT	WT
19	Ad	PL	≥1,000	10-49	WT	WT*	L858R/S768I
20	Ad	PL	≥1,000	<10	WT	WT†	L858R
21	Ad	LN	100-499	≥90	NE	NE	delE746-A750
22	Ad	PL	≥1,000	<10	WT	WT	WT
23	Ad	TBAC	500-999	≥90	DEL	WT	delE746-A750
24	Ad	PL	≥1,000	50-89	WT	WT	WT
25	Ad	PL	100-499	<10	DEL	NE	delE746-A750
26a	Ad	TBAC	500-999	50-89	WT	WT	WT
26b		PL	≥1,000	<10	WT	WT	WT
27	Ad	PAC	≥1,000	50-89	WT	WT	WT
28	Ad	PC	500-999	50-89	DEL	WT	delE746-A750
29	Ad	BC	100-499	50-89	DEL	WT	delE746-A750

Ad, adenocarcinoma; BC, bronchial brushing or washing cytology; DEL, deletional mutation; HRMA, high-resolution melting analysis; LN, fine-needle aspiration cytology of superficial lymph nodes; NE, not evaluable; PAC, percutaneous fine-needle aspiration cytology; PC, pericardial effusion; PL, pleural effusion; Pleo, pleomorphic carcinoma; SCC, squamous cell carcinoma; TBAC, transbronchial fine-needle aspiration cytology; WT, wild type.
* WT after tumor cell–enrichment procedure.
† L858R after tumor cell–enrichment procedure.
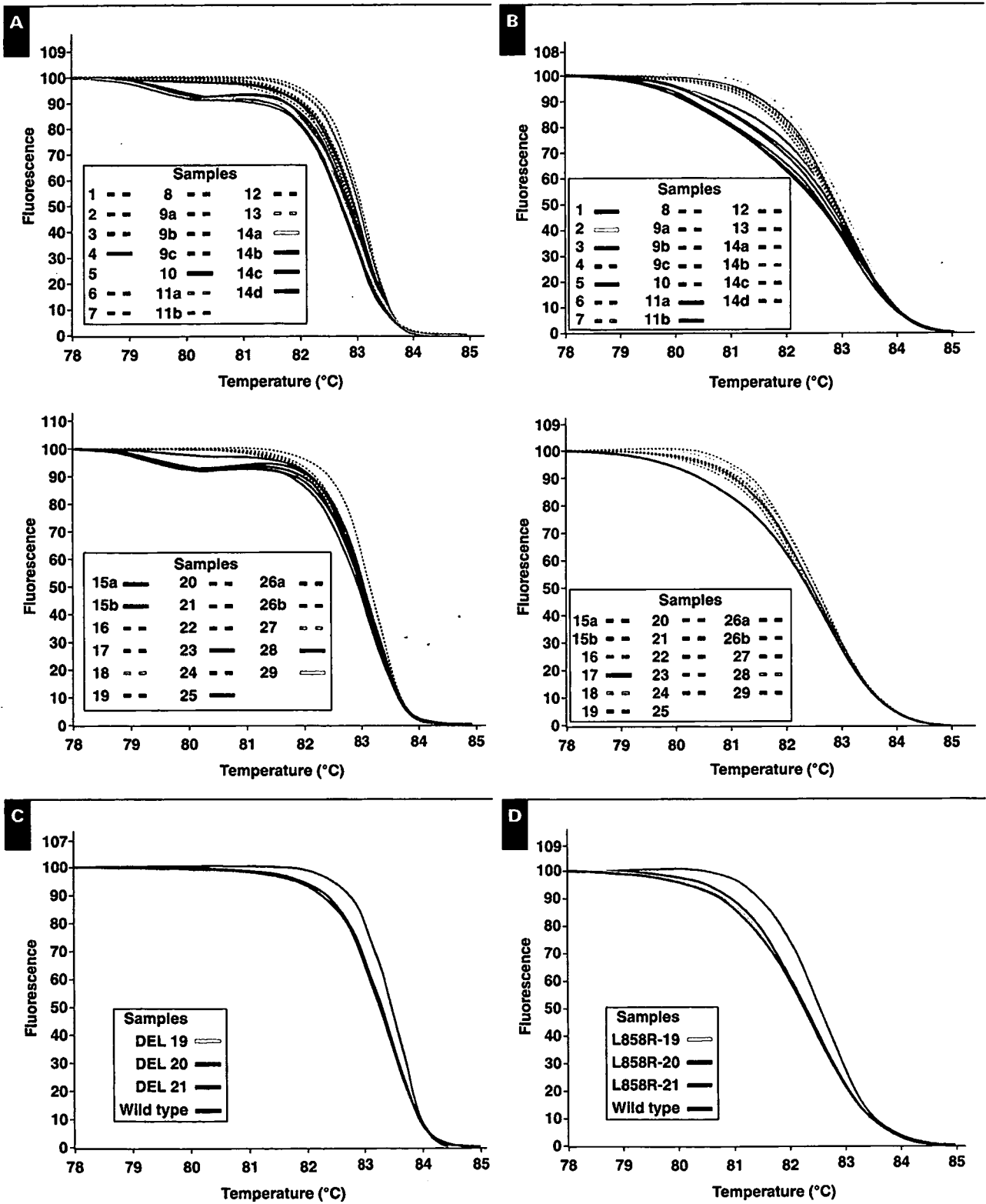
IFigure 2I Adjusted melting curves of DNA extracted from archived cytologic slides in the analysis of epidermal growth factor receptor (*EGFR*) exon 19 (**A**) and exon 21 (**B**). Samples 4, 10, 14a-d, 15a-b, 23, 25, 28, and 29 were identified as containing deletional (DEL) mutations, and samples 1, 2, 3, 5, 11a-b, and 17 were identified as containing the L858R mutations. **C** and **D**, The curves of 3 samples (19-21) are shown in **C** (DEL) and **D** (L858R), but the curves were not obtained in 2 samples (5, DEL; 25, L858R) because of incomplete polymerase chain reaction.

462

surgical specimens from the same patients showed the L858R mutation by direct sequencing. Thus, the results for these samples were considered false-negative. The cytologic appearances of these samples are shown in ▮Image 1▮. Sample 20 contained only a small proportion (<10%) of cancer cells in a background of numerous benign nucleated cells, possibly explaining the false-negative result. In fact, we were able to detect the L858R mutation after tumor cell enrichment by manual dissection in sample 20. However, this was not the case for sample 19, which contained a moderately small proportion (10%-50%) of cancer cells, and the result remained negative even after tumor cell enrichment.

In summary, we identified DEL or L858R in 19 samples (14 patients) and WT *EGFR* in 15 samples (12 patients) accurately by HRMA, but 2 samples (2 patients) gave false-negative results and 1 sample (1 patient) was indeterminate. Accuracy was 92% (34/37) based on the number of samples and 90% (26/29) based on the number of patients. Among the 36 samples in which the genotype was determined, sensitivity was 90% (19/21) and specificity was 100% (15/15), or 88% (14/16) and 100% (12/12), respectively, based on the number of patients. These data indicate that this new method is useful for clinical decision making, especially when a patient is given a positive result.

Discussion

In the present study, we established and validated a new method for detecting 2 major *EGFR* mutations (DEL and L858R) using HRMA for cytologic samples. In a study using a cell line, the sensitivity of HRMA indicated that if at least 10% of cells in a sample were cancer cells, then both DEL and L858R were detectable. L858R was detectable even in 0.1% of L858R cells, whereas DEL could not be detected in 1% of DEL cells. Although the reason for this difference is unclear, the sensitivity is still sufficiently high for application to clinical practice.

We performed the HRMA using archival cytologic samples from 29 patients with NSCLC, and the results were quite consistent with the data obtained for the corresponding 26 cases by LCM plus direct sequencing, which were performed in a previous study.[8] The HRMA was completed in 8 of 9 tumor samples with known DEL mutations, and all 8 samples were identified as having DEL. DEL was detected accurately even in sample 25, in which tumor cells accounted for fewer than 10% of the cells on the slides. In the analysis of archived cytologic samples, no marked difference in detection accuracy was observed between DEL and L858R.

Two samples that contained a relatively small proportion of tumor cells gave false-negative results for L858R; one of these (sample 20) gave a positive result after tumor cell enrichment, but the other (sample 19) did not. The sensitivity of this analysis was 88% (14/16) based on the number of patients, and it increased to 94% (15/16) if tumor cells were enriched in the samples with a small proportion of tumor cells. These results indicate that cytologists will be required not only to diagnose whether samples are benign or malignant but also to evaluate whether they are suitable for molecular analysis.
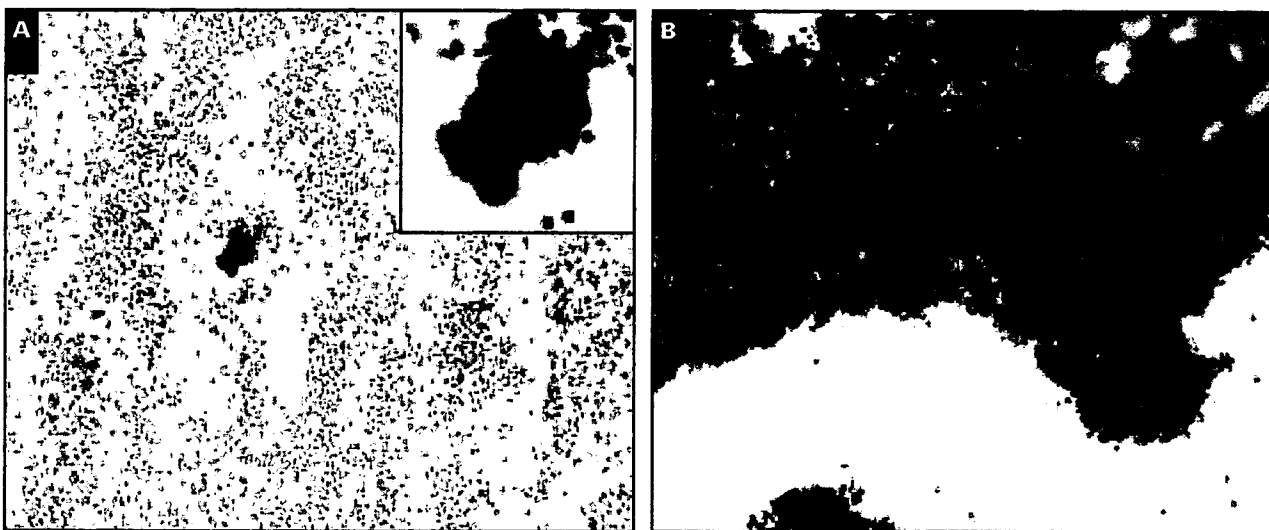
▮Image 1▮ Samples 19 (**A**) and 20 (**B**) show a few cancer cells in a background of many normal nucleated cells. L858R was not detected in these samples by high-resolution melting analysis (HRMA), although direct sequencing showed that DNA extracted from surgical specimens from the same patients had L858R. After retrieving tumor-rich parts selectively, L858R was detected by HRMA from a cytologic slide obtained simultaneously with sample 20, but this was not the case with sample 19 (×10). Insets, The tumor showed 3-dimensional clusters with nuclear atypia compatible with adenocarcinoma (×40).

The mutational status of *EGFR* is a strong predictor of gefitinib sensitivity, and detection of such mutations would provide patients and physicians with important information for optimal choice of therapy. However, mutation detection has not become a common procedure in clinical practice because it often is difficult and impractical. Direct sequencing, which is a standard method for detecting mutations, requires high-quality DNA extracted from an adequate amount of pure tumor cells to obtain precise data and is costly and time-consuming.

Many researchers have tried to establish new methods for detecting *EGFR* mutations using small tumor samples contaminated with normal cells. To date, a number of nonsequencing methods for detecting mutations have been suggested, such as single-strand conformation polymorphism,[15,27] restriction fragment length polymorphism,[28,29] PCR amplification of specific alleles (also known as amplification refractory mutation system and allele specific amplification),[30-32] peptide nucleic acid–mediated PCR clamping,[33,34] peptide nucleic acid–locked nucleic acid PCR clamping,[35] denaturing gradient gel electrophoresis,[36] temperature gradient capillary electrophoresis,[37,38] denaturing high-performance liquid chromatography,[39,40] and high-density oligonucleotide arrays.[41] Some of these methods have been reported to give good results for detection of *EGFR* mutations[15,29,35,40]; however, they often require intensive labor or sophisticated instruments and, therefore, have not been adopted in clinical practice.

HRMA is one of these new methods and has the advantage of being able to distinguish specific mutations from the WT sequence with less labor, time, and cost; PCR and the melting analysis can be performed in the same capillary tube within a few hours, and the running cost is only about $1 (US) per sample.

Detection of DEL and L858R using HRMA is accurate even when archived cytologic samples are used. Because HRMA involves little labor, time, and cost, it is expected to become one of the most practical and useful methods for detecting major *EGFR* mutations in cytologic materials from patients with NSCLC.

References

1. Ozanne B, Richards CS, Hendler F, et al. Over-expression of the EGF receptor is a hallmark of squamous cell carcinomas. *J Pathol.* 1986;149:9-14.
2. Haeder M, Rotsch M, Bepler G, et al. Epidermal growth factor receptor expression in human lung cancer cell lines. *Cancer Res.* 1988;48:1132-1136.
3. Fukuoka M, Yano S, Giaccone G, et al. A multi-institutional randomized phase II trial of gefitinib for previously treated patients with advanced non–small cell lung cancer (the IDEAL 1 Trial). *J Clin Oncol.* 2003;21:2237-2246.
4. Kris MG, Natale RB, Herbst RS, et al. Efficacy of gefitinib, an inhibitor of the epidermal growth factor receptor tyrosine kinase, in symptomatic patients with non–small cell lung cancer: a randomized trial. *JAMA.* 2003;290:2149-2158.
5. Takano T, Ohe Y, Kusumoto M, et al. Risk factors for interstitial lung disease and predictive factors for tumor response in patients with advanced non–small cell lung cancer treated with gefitinib. *Lung Cancer.* 2004;45:93-104.
6. Lynch TJ, Bell DW, Sordella R, et al. Activating mutations in the epidermal growth factor receptor underlying responsiveness of non–small-cell lung cancer to gefitinib. *N Engl J Med.* 2004;350:2129-2139.
7. Paez JG, Janne PA, Lee JC, et al. EGFR mutations in lung cancer: correlation with clinical response to gefitinib therapy. *Science.* 2004;304:1497-1500.
8. Takano T, Ohe Y, Sakamoto H, et al. Epidermal growth factor receptor gene mutations and increased copy numbers predict gefitinib sensitivity in patients with recurrent non–small-cell lung cancer. *J Clin Oncol.* 2005;23:6829-6837.
9. Mitsudomi T, Kosaka T, Endoh H, et al. Mutations of the epidermal growth factor receptor gene predict prolonged survival after gefitinib treatment in patients with non–small cell lung cancer with postoperative recurrence. *J Clin Oncol.* 2005;23:2513-2520.
10. Han S-W, Kim T-Y, Hwang PG, et al. Predictive and prognostic impact of epidermal growth factor receptor mutation in non–small-cell lung cancer patients treated with gefitinib. *J Clin Oncol.* 2005;23:2493-2501.
11. Pao W, Miller V, Zakowski M, et al. EGF receptor gene mutations are common in lung cancers from "never smokers" and are associated with sensitivity of tumors to gefitinib and erlotinib. *Proc Natl Acad Sci U S A.* 2004;101:13306-13311.
12. Kosaka T, Yatabe Y, Endoh H, et al. Mutations of the epidermal growth factor receptor gene in lung cancer: biological and clinical implications. *Cancer Res.* 2004;64:8919-8923.
13. Huang SF, Liu HP, Li LH, et al. High frequency of epidermal growth factor receptor mutations with complex patterns in non–small cell lung cancers related to gefitinib responsiveness in Taiwan. *Clin Cancer Res.* 2004;64:8195-8203.
14. Shigematsu H, Lin L, Takahashi T, et al. Clinical and biological features associated with epidermal growth factor receptor gene mutations in lung cancers. *J Natl Cancer Inst.* 2005;97:339-346.
15. Marchetti A, Martella C, Felicioni L, et al. EGFR mutations in non–small-cell lung cancer: analysis of a large series of cases and development of a rapid and sensitive method for diagnostic screening with potential implications on pharmacologic treatment. *J Clin Oncol.* 2005;23:857-865.
16. Tokumo M, Toyooka S, Kiura K, et al. The relationship between epidermal growth factor receptor mutations and clinicopathologic features in non–small cell lung cancers. *Clin Cancer Res.* 2005;11:1167-1173.

17. Sasaki H, Endo K, Konisi A, et al. EGFR mutation status in Japanese lung cancer patients: genotyping analysis using LightCycler. Clin Cancer Res. 2005;11:2924-2929.

18. Giglio S, Monis PT, Saint CP. Demonstration of preferential binding of SYBR Green I to specific DNA fragments in real-time multiplex PCR. Nucleic Acids Res. 2003;31:e136-e140.

19. Dobrowolski SF, McKinney JT, Filippo CAS, et al. Validation of dye-binding/high-resolution thermal denaturation for the identification of mutations in the SLC22A5 gene. Hum Mutat. 2005;25:306-313.

20. Zhou L, Vandersteen J, Wang L, et al. High-resolution DNA melting curve analysis to establish HLA genotypic identity. Tissue Antigens. 2004;64:156-164.

21. Wittwer CT, Reed GH, Gundry CN, et al. High-resolution genotyping by amplicon melting analysis using LCGreen. Clin Chem. 2003;49(6 pt 1):853-860.

22. Reed GH, Wittwer CT. Sensitivity and specificity of single-nucleotide polymorphism scanning by high-resolution melting analysis. Clin Chem. 2004;50:1748-1754.

23. Carlynn WP, Lester JL, Joseph AH, et al. c-KIT mutation analysis for diagnosis of gastrointestinal stromal tumors in fine needle aspiration specimens. Cancer. 2005;105:165-170.

24. Sordella R, Bell DW, Haber DA, et al. Gefitinib-sensitizing EGFR mutations in lung cancer activate anti-apoptotic pathways. Science. 2004;305:1163-1167.

25. Tracy S, Mukohara T, Hansen M, et al. Gefitinib induces apoptosis in the EGFRL858R non–small-cell lung cancer cell line H3255. Cancer Res. 2004;64:7241-7244.

26. Zhao X, Weir BA, LaFramboise T, et al. Homozygous deletions and chromosome amplifications in human lung carcinomas revealed by single nucleotide polymorphism array analysis. Cancer Res. 2005;65:5561-5570.

27. Orita M, Iwahana H, Kanazawa H, et al. Detection of polymorphisms of human DNA by gel electrophoresis as single-strand conformation polymorphisms. Proc Natl Acad Sci U S A. 1986;86:2766-2770.

28. Felley-Bosco E, Pourzand C, Zijlstra J, et al. A genotypic mutation system measuring mutations in restriction recognition sequences. Nucleic Acids Res. 1991;19:2913-2919.

29. Pan Q, Pao W, Ladanyi M. Rapid polymerase chain reaction–based detection of epidermal growth factor receptor gene mutations in lung adenocarcinomas. J Mol Diagn. 2005;7:396-403.

30. Okayama H, Curiel DT, Brantly ML, et al. Rapid, nonradioactive detection of mutations in the human genome by allele-specific amplification. J Lab Clin Med. 1989;114:105-113.

31. Newton CR, Graham A, Heptinstall LE, et al. Analysis of any point mutation in DNA: the amplification refractory mutation system (ARMS). Nucleic Acids Res. 1989;17:2503-2516.

32. Sarkar G, Cassady J, Bottema CD, et al. Characterization of polymerase chain reaction amplification of specific alleles. Anal Biochem. 1990;186:64-68.

33. Ørum H, Nielsen PE, Egholm M, et al. Single base pair mutation analysis by PNA directed PCR clamping. Nucleic Acids Res. 1993;21:5332-5336.

34. Thiede C, Bayerdorffer E, Blasczyk R, et al. Simple and sensitive detection of mutations in the ras proto-oncogenes using PNA-mediated PCR clamping. Nucleic Acids Res. 1996;24:983-984.

35. Nagai Y, Miyazawa H, Huqun, et al. Genetic heterogeneity of the epidermal growth factor receptor in non–small cell lung cancer cell lines revealed by a rapid and sensitive detection system, the peptide nucleic acid–locked nucleic acid PCR clamp. Cancer Res. 2005;65:7276-7282.

36. Fischer SG, Lerman LS. DNA fragments differing by single base-pair substitutions are separated in denaturing gradient gels: correspondence with melting theory. Proc Natl Acad Sci U S A. 1983;80:1579-1583.

37. Gao Q, Yeung ES. High-throughput detection of unknown mutations by using multiplexed capillary electrophoresis with poly (vinylpyrrolidone) solution. Anal Chem. 2000;72:2499-2506.

38. Li Q, Liu Z, Monroe H, et al. Integrated platform for detection of DNA sequence variants using capillary array electrophoresis. Electrophoresis. 2002;23:1499-1511.

39. Liu W, Smith DI, Rechtzigel KJ, et al. Denaturing high performance liquid chromatography (DHPLC) used in the detection of germline and somatic mutations. Nucleic Acids Res. 1998;26:1396-1400.

40. Jänne PA, Borras AM, Kuang Y, et al. A rapid and sensitive enzymatic method for epidermal growth factor receptor mutation screening. Clin Cancer Res. 2006;12:751-758.

41. Hacia JG, Brody LC, Chee MS, et al. Detection of heterozygous mutations in BRCA1 using high density oligonucleotide arrays and two-colour fluorescence analysis. Nat Genet. 1996;14:441-447.

Dimerization and the signal transduction pathway of a small in-frame deletion in the epidermal growth factor receptor

Kazuko Sakai,[*,§] Tokuzo Arao,[*] Tatsu Shimoyama,[*] Kimiko Murofushi,[§]
Masaru Sekijima,[‖] Naoko Kaji,[‖] Tomohide Tamura,[†]
Nagahiro Saijo,[†] and Kazuto Nishio[*,‡,1]

[*]Shien-Lab, Medical Oncology, [†]National Cancer Center Hospital and [‡]Pharmacology Division,
National Cancer Center Research Institute, Tokyo, Japan; and [§]Department of Biology,
Faculty of Science, Ochanomizu University, Tokyo, Japan; and
[‖]Mitsubishi Chemical Safety Institute Ltd., Ibaraki, Japan

To read the full text of this article, go to http://www.fasebj.org/cgi/doi/10.1096/fj.05-4034fje;
doi: 10.1096/fj.05-4034fje

SPECIFIC AIM

A short, in-frame deletional mutant (E746-A750del) a major mutant form of EGFR in non-small cell lung cancer, and has been reported to be a major determinant of response to EGFR tyrosine kinase inhibitors such as gefitinib and erlotinib. However, the biological and pharmacological functions of mutational EGFR remain unclear. The aim of this study is to clarify whether it is constitutively active or not and whether alteration occurs downstream of the intracellular signaling.

PRINCIPAL FINDINGS

1. A short, in-frame deletional mutant (E746-A750del) induced dimerization and phosphorylation of EGFR without any ligand stimulation

To determine the biological functions of deletion mutant (E746-A750del) EGFR, we used the stable transfected cells of wild-type and deletion mutant of EGFR. Previously, we demonstrated that the 293(D) cells transfected with the deletional EGFR were hypersensitive to EGFR-targeted tyrosine kinase inhibitors such as gefitinib and ZD6474 as compared with the 293(W) cells transfected with wild-type EGFR. Dimerization and phosphorylation of EGFR in these cells were determined by using chemical cross-linker and by immunoblot analysis (Fig. 1). No expression of EGFR dimer or monomer was detected in the 293(M) cells. Increased dimerization and phosphorylation of the deletional EGFR with a molecular weight of ~400 kDa were detected without EGF stimulation in the 293(D) cells. When stimulated with the EGF, increased dimerized and phosphorylated EGFR were observed in the 293(W) cells, whereas no response of EGFR to EGF was

observed in the 293(D) cells. The ratio of dimerized to monomeric EGFR in 293(W) and 293(D) cells was analyzed densitometrically (Fig. 1, right). The dimer/monomer ratio in the 293(W) cells was markedly increased (~3-fold) by addition of EGF. Under unstimulated conditions, the dimer/monomer ratio of the 293(D) cells was higher than that of the 293(W) cells and the ratio was unchanged by addition of EGF. These results suggest that the cells expressing the wild-type of EGFR responded to EGF for their dimerization and phosphorylation and that the deletional mutant of EGFR was dimerized and phosphorylated constitutively without any ligand stimulation.

2. p44/42 MAPK and AKT pathways are activated in the cells expressing deletional EGFR without ligand stimulation

We examined the phosphorylation status of p44/42 MAPK and AKT that are major downstream targets of EGFR in the transfectants. Even under unstimulated conditions, increased phosphorylation of p44/42 MAPK and AKT was observed in the 293(D) cells. In the 293(W) cells, increased phosphorylation of p44/42 MAPK and AKT was observed with the addition of EGF but p44/42 MAPK was remarkably phosphorylated. On the other hand, no increased phosphorylation of p44/42 MAPK and AKT was observed with the addition of EGF in the 293(D) cells. This result suggests that the p44/42 MAPK and AKT pathways are activated in cells expressing the deletional EGFR without ligand stimulation.

---

[1] Correspondence: Shien-Lab, Medical Oncology, National Cancer Center Hospital, Tsukiji 5-1-1, Chuo-ku, Tokyo 104-0045, Japan. E-mail: knishio@gan2.res.ncc.go.jp
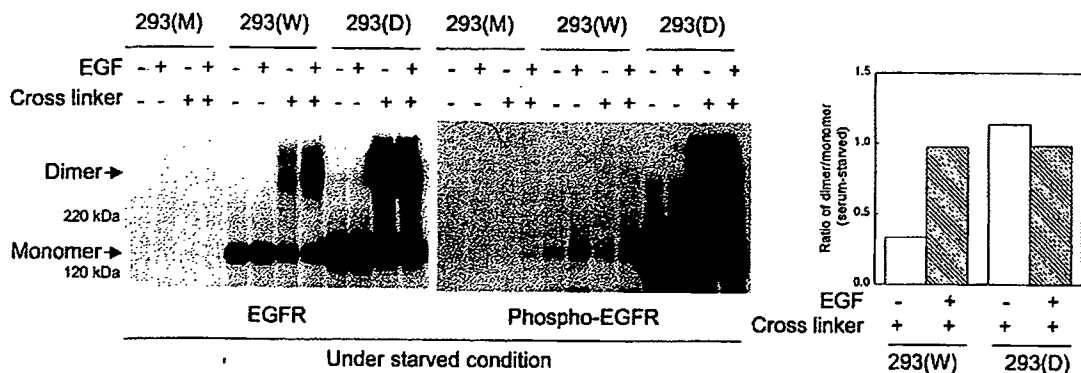
Figure 1. Dimerization and phosphorylation of wild-type EGFR and deletional EGFR A. The 293 cells transfected with the empty vector (293(M)), wild-type EGFR (293(W)), and deletional EGFR (293(D)) were treated with or without EGF (10 ng/mL) for 10 min after serum starvation. After two washes with ice-cold PBS(+), monolayer cells were incubated with the chemical cross-linking reagent BS³ (1.5 mM) in PBS(+). Glycine (20 mM) was added for an additional 5 min to terminate the reaction. The lysates (twenty μg protein) were subjected to 2–15% SDS-PAGE followed by immunoblot analysis using anti-EGFR and anti-phospho-EGFR. Right panel: ratio of dimerized to monomeric EGFR.

3. Gefitinib inhibited the AKT signaling pathway more strongly than the p44/42 MAPK signaling pathway

We next determined the action of EGFR-targeted tyrosine kinase inhibitor gefitinib on downstream of deletional EGFR (Fig. 2A). In the 293(W) cells, phosphorylation of p44/42 MAPK was not inhibited by exposure to a low dose of gefitinib (0.01 μM) but phosphorylation of AKT was inhibited by exposure to gefitinib (~70%, Fig. 2C). In contrast, exposure to gefitinib decreased phospho-EGFR in the 293(D) cells. Phosphorylation of AKT was completely inhibited by 0.01 μM gefitinib exposure (~99%, Fig. 2C), whereas inhibition of p44/42 MAPK phosphorylation was not remarkable in the 293(D) cells (~20%, Fig. 2B). These data suggest that gefitinib inhibited the AKT signaling pathway more strongly than the p44/42 MAPK signaling pathway in the cells expressing the deletion mutant EGFR.

## 4. AKT pathway was activated in the PC-9 cells expressing deletional EGFR intrinsically

To examine whether increased phosphorylation is also observed in the lung cancer cells intrinsically expressing deletional EGFR, we monitored the phosphorylation of EGFR and its related molecules in the PC-9 cells expressing deletional EGFR by using a beads-based mulitiplex assay. We found increased phosphorylation of EGFR and downstream molecules of AKT pathway including IκB-α in PC-9 cells. This finding is consistent with the result of the previous experiments with the 293(D) cells. It is suggested that AKT pathway is activated in the cells expressing deletional EGFR intrinsically.

CONCLUSIONS AND SIGNIFICANCE

To clarify the function of deletional EGFR, we used the cell transfectants with deletional EGFR [293(D)] that is

Figure 2. Effect of gefitinib on phosphorylation of EGFR, p44/42 MAPK, and AKT in the EGFR transfected 293 cells. A) The 293(M), 293(W), and 293(D) cells were incubated with gefitinib (0.01 μM) for 3 h or 12 h under nonstarved conditions. After two washes with ice-cold PBS(+), monolayer cells were lysed. Equivalent amounts of protein were separated by 2–15% gradient SDS-PAGE for EGFR or 10–20% for p44/42 MAPK, phospho-p44/42 MAPK, AKT, and phospho-AKT, then subjected to immunoblot analysis. B) Histogram of the degree of p44/42 MAPK activation expressed as phospho-p44/42 MAPK per total p44/42 MAPK. C) Histogram of the degree of AKT activation expressed as phospho-AKT per total AKT.

467

Wild-type EGFR **Deletion-mutant EGFR**

Survival
Cell proliferation
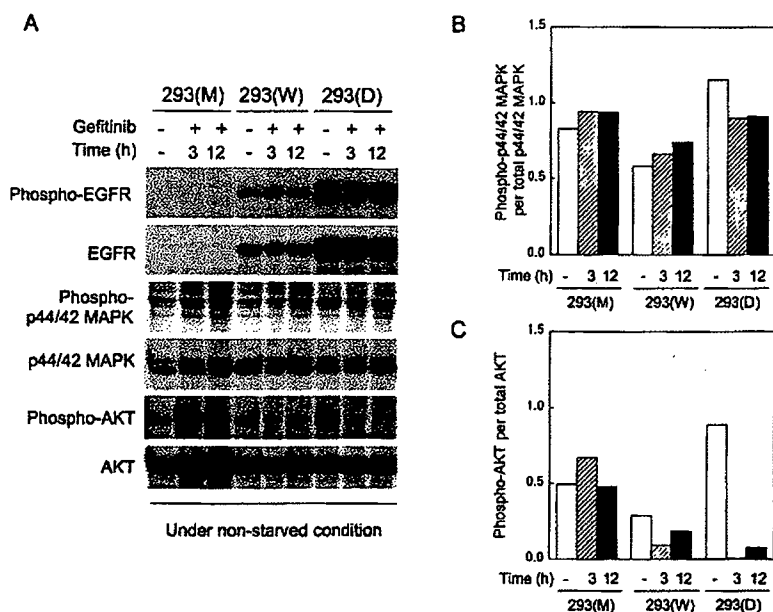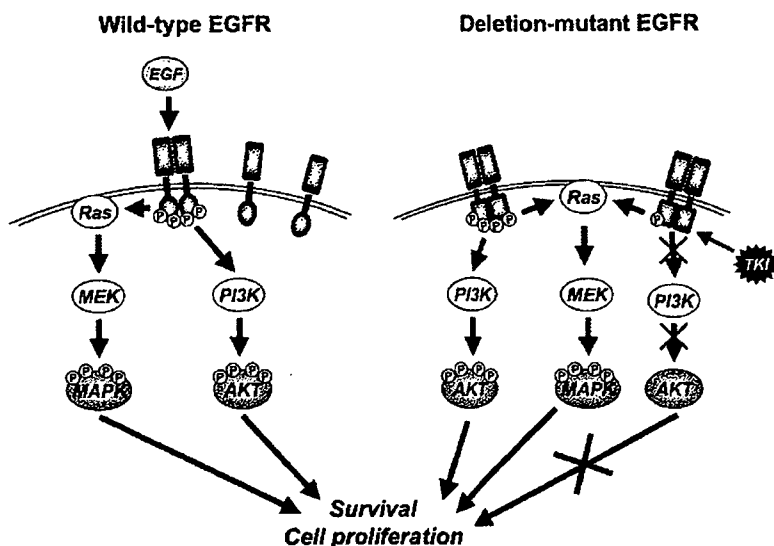
Figure 3. Function of deletional EGFR. Wild-type EGFR is dimerized and phosphorylated by EGF the wild-type EGFR and MAPK and AKT pathways are activated. The deletion mutant EGFR is dimerized and phosphorylated without EGF. Both MAPK and AKT pathways are activated; but phospho-AKT was inhibited by TKI predominantly in the cells expressing deletional EGFR. MEK, MAP kinase/extracellular regulated kinases; PI3K, phosphoinositide-3-kinase; TKI, tyrosine kinase inhibitors.

hypersensitive to tyrosine kinase inhibitors (e.g., gefitinib). We detected significantly higher levels of dimerization and phosphorylation of deletional EGFR without any ligand stimulation in the cells deletional EGFR. Increased phosphorylation of p44/42 MAPK and AKT was observed in the 293(D) cells. These results suggest that deletional EGFR is constitutively active. When the 293(D) cells were exposed to gefitinib (0.01 μM), AKT phosphorylation was completely suppressed, suggesting that deletional EGFR signaling inclines toward the AKT pathways. A summary of characteristics of deletional EGFR is shown in **Fig. 3**.

An additional experiment using a PC-9 lung cancer cell line intrinsically expressing deletional EGFR confirmed the gain of function of deletional EGFR and activated AKT signaling pathway.

Results from this study have provided the understanding for biological functions of deletional EGFR and cellular hypersensitivity to the EGFR-targeted tyrosine kinase inhibitor.

Now over 30 types of mutation have been reported in clinical lung cancer specimens. We will examine the biological function of other types of EGFR mutants differentially, with the aim of selecting clinically meaningful mutations. 🗾

Docetaxel Consolidation Therapy Following Cisplatin, Vinorelbine, and Concurrent Thoracic Radiotherapy in Patients with Unresectable Stage III Non-small Cell Lung Cancer

Ikuo Sekine, Hiroshi Nokihara,* Minako Sumi,† Nagahiro Saijo,‡ Yutaka Nishiwaki,§ Satoshi Ishikura,|| Kiyoshi Mori,¶ Iwao Tsukiyama,# and Tomohide Tamura**

Background: To evaluate the feasibility and efficacy of docetaxel consolidation therapy after concurrent chemoradiotherapy for unresectable stage III non–small cell lung cancer (NSCLC).

Patients and Methods: The eligibility criteria included unresectable stage III NSCLC, no previous treatment, age between 20 and 74 years, and performance status 0 or 1. Treatment consisted of cisplatin (80 mg/m^2 on days 1, 29, and 57), vinorelbine (20 mg/m^2 on days 1, 8, 29, 36, 57, and 64), and thoracic radiotherapy (TRT) (60 Gy/30 fractions over 6 weeks starting on day 2), followed by consolidation docetaxel (60 mg/m^2 every 3 to 4 weeks for three cycles).

Results: Of 97 patients who were enrolled in this study between 2001 and 2003, 93 (76 males and 17 females with a median age of 60) could be evaluated. Chemoradiotherapy was well tolerated; three cycles of chemotherapy and 60 Gy of TRT were administered in 80 (86%) and 87 (94%) patients, respectively. Grade 3 or 4 neutropenia, esophagitis, and pneumonitis developed in 62, 11, and 3 patients, respectively. Docetaxel consolidation was administered in 59 (63%) patients, but three cycles were completed in only 34 (37%) patients. The most common reason for discontinuation was pneumonitis, which developed in 14 (24%) of the 59 patients. During consolidation therapy, grade 3 or 4 neutropenia, esophagitis, and pneumonitis developed in 51, 2, and 4 patients, respectively. A total of four patients died of pneumonitis. We calculated a V_{20} (the percent volume of the normal lung receiving 20 Gy or more) on a dose-volume histogram in 25 patients. Of these, five patients developed grade 3 or more severe radiation pneumonitis. A median V_{20} for these five patients was 35% (range, 26–40%), whereas the median V_{20} for the remaining 20 patients was 30% (range, 17–35%) ($p =$ 0.035 by a Mann–Whitney test). The response rate was 81.7% (95% confidence interval [CI], 72.7–88.0%), with 5 complete and 71 partial responses. The median progression-free survival was 12.8 (CI, 10.2–15.4) months, and median survival was 30.4 (CI, 24.5–36.3) months. The 1-, 2-, and 3-year survival rates were 80.7, 60.2, and 42.6%, respectively.

Conclusion: This regimen produced promising overall survival in patients with stage III NSCLC, but the vast majority of patients could not continue with the docetaxel consolidation because of toxicity.

Key Words: Non-small cell lung cancer, Chemoradiotherapy, Consolidation, Docetaxel.

(J Thorac Oncol. 2006;1: 810–815)

Divisions of *Internal Medicine and Thoracic Oncology, and †Radiation Oncology, National Cancer Center Hospital, Tokyo, Japan; Divisions of ‡Internal Medicine, §Thoracic Oncology, and ||Radiation Oncology, National Cancer Center Hospital East, Kashiwa, Japan; and Divisions of ¶Thoracic Oncology and #Radiotherapy, Tochigi Cancer Center, Utsunomiya, Japan.

Address for correspondence: Ikuo Sekine, Division of Thoracic Oncology and Internal Medicine, National Cancer Center Hospital, Tsukiji 5-1-1, Chuo-ku, Tokyo 104-0045, Japan. E-mail: isekine@ncc.go.jp

Locally advanced unresectable non–small cell lung cancer (NSCLC), stage IIIA with bulky N2 and stage IIIB disease without pleural effusion, is characterized by large primary lesions and/or involvement of the mediastinal or supraclavicular lymph nodes and occult systemic micrometastases. A combination of thoracic radiotherapy and chemotherapy is the standard medical treatment for this disease, but the optimal combination has not been established.[1] Although the available data are insufficient to accurately define the size of a potential benefit,[2] concurrent chemoradiotherapy using a platinum doublet has been shown to be superior to the sequential approach in phase III trials of this disease.[3–5] However, third-generation cytotoxic agents, which have provided better patient survival with extrathoracic spread than the old-generation agents, must be reduced when administered concurrently with thoracic radiotherapy.[6] Thus, it has been hypothesized that the addition of systemic dose chemotherapy with a new cytotoxic agent to concurrent chemoradiotherapy, either as induction or as consolidation chemotherapy, might further improve patient survival.[1]

The consolidation chemotherapy with docetaxel was based on the observation that this drug was highly active in the primary treatment of metastatic NSCLC, producing a response rate (RR) as high as 20% after platinum-based chemotherapy failed.[7–9] Highly encouraging results of a me-

dian survival time (MST) of more than 2 years and a 3-year survival rate of nearly 40% were obtained in a phase II trial of docetaxel consolidation after chemoradiotherapy with cisplatin and etoposide in patients with stage IIIB NSCLC (SWOG study S9504).[10]

We have developed a combination chemotherapy schedule with cisplatin and vinorelbine concurrently administered with thoracic radiotherapy at a total dose of 60 Gy in 30 fractions in patients with unresectable stage III NSCLC. The results of a phase I study in 18 patients were very promising, with a RR of 83%, a MST of 30 months, and a 3-year survival rate of 50%.[6] Thus, addition of docetaxel consolidation to this regimen is a particularly interesting therapeutic strategy. The objectives of the current study were to evaluate the feasibility of docetaxel consolidation therapy after concurrent chemoradiotherapy with cisplatin and vinorelbine and to evaluate the efficacy and safety of the whole treatment regimen including both the chemoradiotherapy and consolidation therapy in patients with unresectable stage IIIA and IIIB NSCLC.

PATIENTS AND METHODS

Patient Selection

The eligibility criteria were histologically or cytologically proven NSCLC; unresectable stage IIIA or IIIB disease; no previous treatment; measurable disease; tumor within an estimated irradiation field no larger than half the hemithorax; age between 20 and 74 years; Eastern Cooperative Oncology Group performance status (PS) of 0 or 1; adequate bone marrow function (12.0 × 10^9/liter ≥ white blood cell [WBC] count ≥4.0 × 10^9/liter, neutrophil count ≥2.0 × 10^9/liter, hemoglobin ≥10.0 g/dl, and platelet count ≥100 × 10^9/liter), liver function (total bilirubin ≤1.5 mg/dl and transaminase no more than twice the upper limit of the normal value), and renal function (serum creatinine ≤1.5 mg/dl and creatinine clearance ≥60 ml per minute); and a PaO_2 of 70 torr or more under room air conditions. Patients were excluded if they had malignant pleural or pericardial effusion, active double cancer, a concomitant serious illness such as uncontrolled angina pectoris, myocardial infarction in the previous 3 months, heart failure, uncontrolled diabetes mellitus, uncontrolled hypertension, interstitial pneumonia or lung fibrosis identified by a chest x-ray, chronic obstructive lung disease, infection or other diseases contraindicating chemotherapy or radiotherapy, pregnancy, or if they were breast feeding. All patients gave their written informed consent.

Pretreatment Evaluation

The pretreatment assessment included a complete blood cell count and differential count, routine chemistry determinations, creatinine clearance, blood gas analysis, electrocardiogram, lung function testing, chest x-rays, chest computed tomographic (CT) scan, brain CT scan or magnetic resonance imaging, abdominal CT scan or ultrasonography, and radionuclide bone scan.

Treatment Schedule

Treatment consisted of a chemoradiotherapy phase with three cycles of cisplatin and vinorelbine followed by a con-
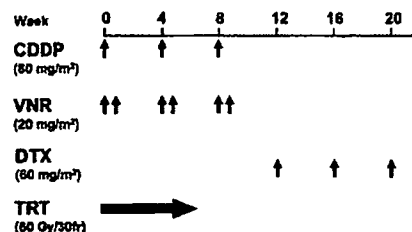

FIGURE 1. Treatment schema. CDDP, cisplatin; DTX, docetaxel; TRT, thoracic radiotherapy; VNR, vinorelbine.

solidation phase with three cycles of docetaxel (Figure 1). Cisplatin 80 mg/m^2 was administered on days 1, 29, and 57 by intravenous infusion for 60 minutes with 2500 to 3000 ml of fluid for hydration. Vinorelbine diluted in 50 ml of normal saline was administered intravenously on days 1, 8, 29, 36, 57, and 64. All patients received prophylactic antiemetic therapy consisting of a $5HT_3$-antagonist and a steroid.

Radiation therapy was delivered with megavoltage equipment (≥6 MV) using anterior/posterior opposed fields up to 40 Gy in 20 fractions including the primary tumor, the metastatic lymph nodes, and the regional nodes. A booster dose of 20 Gy in 10 fractions was given to the primary tumor and the metastatic lymph nodes for a total dose of 60 Gy using bilateral oblique fields. A CT scan–based treatment planning was used in all patients. The clinical target volume (CTV) for the primary tumor was defined as the gross tumor volume (GTV) plus 1 cm taking account of subclinical extension. CTV and GTV for the metastatic nodes (>1 cm in shortest dimension) were the same. Regional nodes, excluding the contralateral hilar and supraclavicular nodes, were included in the CTV, but the lower mediastinal nodes were included only if the primary tumor was located in the lower lobe of the lung. The planning target volumes for the primary tumor, the metastatic lymph nodes, and regional nodes were determined as CTVs plus 0.5- to 1.0-cm margins laterally and 1.0- to 2.0-cm margins craniocaudally, taking account of setup variations and internal organ motion. Lung heterogeneity corrections were not used.

The criteria for starting consolidation chemotherapy were completion of three cycles of cisplatin and vinorelbine and a full dose of thoracic radiotherapy, the absence of progressive disease, adequate general condition within 6 weeks of the start of the third cycle of cisplatin and vinorelbine (PS 0 or 1, WBC count ≥3.0 × 10^9/liter, neutrophil count ≥1.5 × 10^9/liter, hemoglobin ≥9.0 g/dl and platelet count ≥100 × 10^9/liter, total bilirubin ≤1.5 mg/dl and transaminase no more than twice the upper limit of the normal value, and a PaO_2 of 70 torr or more at room air). Docetaxel (60 mg/m^2) was administered intravenously for 1 hour every 3 to 4 weeks for three cycles.

Toxicity Assessment and Treatment Modification

Complete blood cell counts and differential counts, routine chemistry determinations, and a chest x-ray were performed once a week during the course of treatment. Acute toxicity was graded according to the NCI Common Toxicity Criteria, and late toxicity associated with thoracic radiother-

811

apy was graded according to the Radiation Therapy Oncology Group/European Organization for Research and Treatment of Cancer late radiation morbidity scoring scheme. Vinorelbine administration on day 8 was omitted if any of the following were noted: WBC count $<3.0 \times 10^9$/liter, neutrophil count $<1.5 \times 10^9$/liter, platelet count $<100 \times 10^9$/liter, elevated hepatic transaminase level or total serum bilirubin of at least grade 2, fever $\geq 38°C$, or PS ≥ 2. Subsequent cycles of cisplatin and vinorelbine chemotherapy were delayed if any of the following toxicities were noted on day 1: WBC count $<3.0 \times 10^9$/liter, neutrophil count $<1.5 \times 10^9$/liter, platelet count $<100 \times 10^9$/liter, serum creatinine level ≥ 1.6 mg/dl, elevated hepatic transaminase level or total serum bilirubin of at least grade 2, fever $\geq 38°C$, or PS ≥ 2. The dose of cisplatin was reduced by 25% in all subsequent cycles if the serum creatinine level rose to 2.0 mg/dl or higher. The dose of vinorelbine or docetaxel was reduced by 25% in all subsequent cycles if any of the following toxicities were noted: WBC count $<1.0 \times 10^9$/liter, platelet count $<10 \times 10^9$/liter, or grade 3 or 4 infection or liver dysfunction. Thoracic radiotherapy was suspended if any of the following were noted: fever $\geq 38°C$, grade 3 esophagitis, PS of 3, or PaO_2 <70 torr. Thoracic radiotherapy was terminated if any of the following were noted: grade 4 esophagitis, grade 3 or 4 pneumonitis, PS of 4, or duration of radiotherapy of over 60 days. The use of granulocyte colony-stimulating factor during radiotherapy was not permitted unless radiotherapy was on hold. The criteria for termination of docetaxel consolidation were not defined in the protocol.

Response Evaluation

Objective tumor response was evaluated according to the Response Evaluation Criteria in Solid Tumor.[11] Local recurrence was defined as tumor progression in the primary site and in the hilar, mediastinal, and supraclavicular lymph nodes after a partial or complete response; regional recurrence as the development of malignant pleural and pericardial effusions; and distant recurrence as the appearance of a distant metastasis.

Study Design, Data Management, and Statistical Considerations

This study was conducted at three institutions: the National Cancer Center Hospital, National Cancer Center Hospital East, and Tochigi Cancer Center. The protocol and consent form were approved by the institutional review board of each institution. Registration was conducted at the registration center. Data management, periodic monitoring, and the final analysis were performed by the study coordinator.

The primary objective of the current study was to evaluate the feasibility of docetaxel consolidation therapy. The secondary endpoints were toxicity observed during chemoradiotherapy and consolidation therapy, the best response, and overall survival in all patients eligible to participate in this study. Because no standard method to evaluate consolidation chemotherapy after chemoradiotherapy has been established, we arbitrarily defined the primary endpoint of this study as a ratio (R) of the number of patients receiving docetaxel without grade 4 nonhematological toxicity or treat-

ment-related death to the total number of patients receiving docetaxel. The sample size was initially estimated to be 34 patients with a power of 0.80 at a significance level of 0.05, under the assumption that a R of 0.95 would indicate potential usefulness, whereas a R of 0.8 would be the lower limit of interest, and that 85% of patients would move into the consolidation phase. An analysis of the first 13 patients, however, showed that only 8 (61%) patients advanced into the consolidation phase. The reasons for not receiving docetaxel were disease progression in one, delay in completion of chemoradiotherapy in two, grade 3 esophagitis in one, and death due to hemoptysis in one patient. Considering that the SWOG trial S9504 included 83 patients, we decided to revise the number of patients in the current study. According to Simon's two-stage minimax design, the required number of patients was calculated to be 59 with a power of 0.80 at a significance level of 0.05, under the assumption that a R of 0.85 would indicate potential usefulness, whereas a R of 0.7 would be the lower limit of interest.[12] Assuming that 61% of registered patients would move into the consolidation phase, the sample size was determined to be 97 patients.

Overall survival time and progression-free survival time were estimated by the Kaplan–Meier method, and confidence intervals (CI) were based on Greenwood's formula.[13] Overall survival time was measured from the date of registration to the date of death (from any cause) or to the last follow-up. Progression-free survival time was measured from the date of registration to the date of disease progression, death (from any cause), or the last follow-up. Patients who were lost to follow-up without event were censored at the date of their last known follow-up. A CI for RR was calculated using methods for exact binomial CIs. The Dr. SPSS II 11.0 for Windows software package (SPSS Japan Inc., Tokyo, Japan) was used for statistical analyses.

RESULTS

Registration and Characteristics of the Patients

A total of 97 patients were enrolled in this study between April 2001 and June 2003. Four patients were excluded from this study before the treatment was started because the radiation treatment planning disclosed that their tumors were too advanced for curative thoracic radiotherapy. Thus, 93 patients who received the protocol-defined treatment were the subjects of this analysis (Figure 2). There were 76 males and 17 females, with a median age of 60 (range 31–74). Body weight loss was less than 5% in 77 patients; adenocarcinoma histology was noted in 57 patients, and stage IIIA disease was noted in 41 patients (Table 1).

Treatment Delivery

Treatment delivery was generally well maintained in the chemoradiotherapy phase (Table 2). Full cycles of cisplatin and vinorelbine and the full dose of thoracic radiotherapy were administered in 80 (86%) and 87 (94%) patients, respectively. Delay in radiotherapy was less than 5 days in 61 (66%) patients. In contrast, the delivery of docetaxel was poor (Table 2). A total of 59 (63%) patients could enter the consolidation phase, and only 34 (37%) patients completed three cycles of docetaxel chemotherapy. The reasons for not
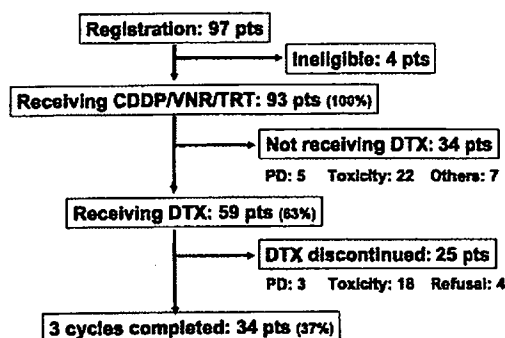
FIGURE 2. Patient registration. CDDP, cisplatin; DTX, docetaxel; TRT, thoracic radiotherapy; VNR, vinorelbine.

receiving consolidation were toxicity in 22 (65%) patients including pneumonitis in seven patients, myelosuppression in five patients, esophagitis in four patients, liver dysfunction in two patients, infection in two patients, other toxicity in two patients, progressive disease in five (15%) patients, patient refusal in three (9%) patients, early death due to hemoptysis in one (3%) patient, and other reasons in three (9%) patients. Of the 59 patients, 18 (31%) discontinued docetaxel consolidation because of toxicity, including pneumonitis ($n = 14$) and esophagitis, infection, gastric ulcer, and allergic reaction ($n = 1$ each), four (7%) because of patient refusal, and three (5%) because of progressive disease.

Toxicity

Acute severe toxicity in the chemoradiotherapy phase was mainly leukopenia and neutropenia, whereas grade 3 or 4 thrombocytopenia was not noted (Table 3). Severe nonhematological toxicity was sporadic, and grade 3 esophagitis and pneumonitis were observed in only 11 (12%) and 3 (3%) patients, respectively. Acute severe toxicity in the consolidation phase also consisted of neutropenia and associated in-

TABLE 1. Patient Characteristics

Characteristics	n	%
Gender		
Male	76	82
Female	17	18
Age median (range)	60	31–74
Weight loss		
<5%	76	81
5–9%	12	13
≥10%	3	3
Unknown	2	2
Histology		
Adenocarcinoma	57	61
Squamous cell carcinoma	23	25
Large cell carcinoma	12	13
Others	1	1
Stage		
IIIA	41	44
IIIB	52	56

TABLE 2. Treatment Delivery

Variables	n	%
Cisplatin and vinorelbine chemotherapy		
Total number of cycles		
3	80	86
2	10	11
1	3	3
Number of vinorelbine skips		
0	63	68
1	25	27
2–3	5	5
Thoracic radiotherapy		
Total dose (Gy)		
60	87	94
50–59	4	4
<50	2	2
Delay (days)		
<5	61	66
5–9	20	22
10–16	6	6
Not evaluable (<60 Gy)	6	6
Docetaxel consolidation		
Number of cycles		
3	34	37
2	12	13
1	13	14
0	34	34

fection (Table 4). In addition, grade 3 or 4 pneumonitis developed in 4 (7%) patients. The R observed in this study was 0.05 (3 out of 57 patients), which was much lower than the hypothetical value. Grade 3 or 4 late toxicities were included lung toxicity in four patients, esophageal toxicity in two patients, renal toxicity in one patient, and a second esophageal cancer that developed 35.4 months after the start of the chemoradiotherapy in one patient. Treatment-related

TABLE 3. Acute Toxicity in Chemoradiotherapy ($n = 93$)

Toxicity	Grade 3	Grade 4	3 + 4	%
Leukopenia	54	18	72	77
Neutropenia	33	29	62	67
Anemia	21	0	21	23
Infection	15	1	16	17
Esophagitis	11	0	11	12
Hyponatremia	11	0	11	12
Anorexia	9	1	10	11
Nausea	5	—	5	5
Pneumonitis	3	0	3	3
Syncope	2	0	2	2
Hyperkalemia	2	0	2	2
Ileus	0	1	1	1
Cardiac ischemia	1	0	1	1

813

TABLE 4. Acute Toxicity in Consolidation Therapy (*n* = 57)

Toxicity	Grade			%
	3	4	3 + 4	
Leukopenia	33	11	44	77
Neutropenia	24	26	50	88
Anemia	5	0	5	9
Infection	5	1	6	11
Esophagitis	2	0	2	3
Anorexia	1	0	1	2
Pneumonitis	2	2	4	7

death was observed in four (4%) patients. Of these, three received docetaxel, and one did not. The reason for death was pneumonitis in all patients. We calculated a V_{20} (the percent volume of the normal lung receiving 20 Gy or more) on a dose–volume histogram in 25 patients. Of these, five patients developed grade 3 or severer radiation pneumonitis. A median V_{20} for these five patients was 35% (range, 26–40%), whereas that for the remaining 20 patients was 30% (range, 17–35%) (*p* = 0.035 by a Mann–Whitney test).

Objective Responses, Relapse Pattern, and Survival

All 93 patients were included in the analyses of tumor response and survival. Complete and partial responses were obtained in 5 (5%) and 71 patients (76%), respectively, for an overall RR of 81.7% (95% CI, 72.7–88.0%). Stable and progressive diseases occurred in 12 (13%) and 5 (5%) patients, respectively. With a median follow-up period of 29.7 months, 38 patients developed locoregional recurrence, 32 developed distant recurrence, 4 developed both locoregional and distant recurrences, and 19 did not. The median progression-free survival time was 12.8 (95% CI, 10.2–15.4) months (Figure 3). Two patients underwent salvage surgery for a recurrent primary tumors. Conventional chemotherapy and gefitinib monotherapy were administered after recurrence in 20 and 25 patients, respectively. The median overall survival time was 30.4 (95% CI,
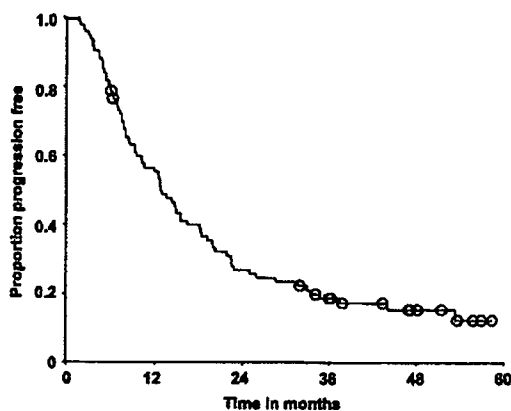

FIGURE 3. Progression-free survival (*n* = 93). The median progression-free survival time was 12.8 (95% CI, 10.2–15.4) months.
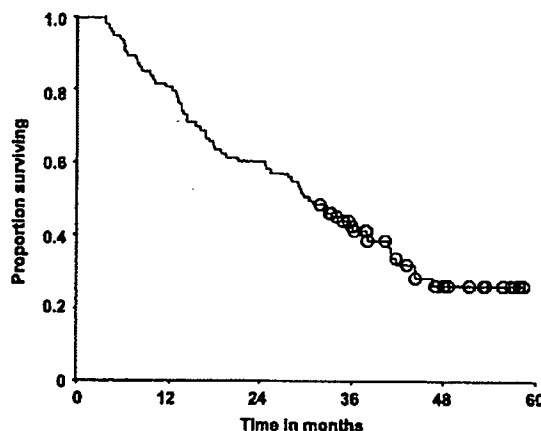

FIGURE 4. Overall survival (*n* = 93). The median overall survival time was 30.4 (95% CI, 25.4–35.4) months. The 1-, 2-, and 3-year survival rates were 80, 60, and 40%, respectively.

24.5–36.3) months. The 1-, 2-, and 3-year survival rates were 80.7, 60.2, and 42.6%, respectively. (Figure 4).

DISCUSSION

This study showed that concurrent chemoradiotherapy with cisplatin, vinorelbine, and standard thoracic radiotherapy was well tolerated, with a high completion rate exceeding 80%. The incidence of acute toxicity, including 67% (62/93) of grade 3 or 4 neutropenia, 12% (11/93) of grade 3 esophagitis, and 3% (3/93) of grade 3 pneumonitis, were comparable with other reports of concurrent chemoradiotherapy.[3,4,10] In contrast, consolidation docetaxel could be administered in only 59 of 93 (63%) patients eligible to participate in this study. Of the remaining 34 patients, 22 (65%) patients did not receive consolidation chemotherapy because of toxicities affecting various organs. Other studies also showed that not all patients proceeded to the consolidation phase after completion of concurrent chemoradiotherapy: 61 to 78% of patients after two cycles of cisplatin and etoposide with radiotherapy,[3,10] and 54 to 75% of patients after weekly carboplatin and paclitaxel with radiotherapy.[14,15] Thus, for 20 to 40% of the patients, concurrent chemoradiotherapy was as much as they could undergo, and the additional chemotherapy was not practical.

Furthermore, the number of patients who fulfilled the three cycles of consolidation docetaxel was only 34 (58%) of the 59 patients, which corresponded to only 37% of those eligible in this study. The reason for the termination of docetaxel in the 25 patients was toxicity in 18 (72%) patients, especially pneumonitis in 14 (56%) patients. The grade of pneumonitis during the consolidation phase was within grade 2 in most cases, and this was probably because docetaxel was discontinued early. Considering that pneumonitis associated with cancer treatment is more common in Japan, docetaxel consolidation is not thought to be feasible in the Japanese population. The MST and the 3-year survival rate in all eligible patients were 33 months and 44% in this study, but docetaxel consolidation was unlikely to contribute to these promising results because only 37% of patients received full cycles of docetaxel. This contrasts clearly with the result of

814

the SWOG study S9504, a phase II trial of two cycles of cisplatin and etoposide with thoracic radiation followed by three cycles of docetaxel. In this trial, 75% of patients starting consolidation and 59% of those entering the trial received full cycles. In addition, docetaxel consolidation seemed to prolong survival, although this was drawn from a retrospective comparison of the results between the two SWOG studies S9504 and S9019.[10]

There is no widely used' definition of consolidation therapy following chemoradiotherapy. Given that consolidation therapy is arbitrarily defined as chemotherapy with three cycles or more after the completion of concurrent chemoradiotherapy, only one randomized trial is available in the literature. The randomized phase III trial of standard chemoradiotherapy with carboplatin and paclitaxel followed by either weekly paclitaxel or observation in patients with stage III NSCLC showed that only 54% of patients proceeded to randomization, and overall survival was worse in the consolidation arm (MST, 16 versus 27 months).[15] Thus, there have been no data supporting the use of consolidation therapy, especially when a third-generation cytotoxic agent such as paclitaxel and vinorelbine is incorporated into concurrent chemoradiation therapy.

The low complete-response rate of 5% in this study may be explained partly by an inability to distinguish between inactive scarring or necrotic tumor and active tumor after radiotherapy. Positron emission tomography (PET) using 18F-fluorodeoxyglucose showed a much higher rate of complete response than conventional CT scanning and provided a better correlation of the response assessment using PET with patterns of failure and patient survival.[16] In addition, the high locoregional relapse rate in this study clearly showed that the conventional total dose of 60 Gy was insufficient. Three-dimensional treatment planning, omission of elective nodal irradiation, and precise evaluation of the gross tumor volume by PET may facilitate the escalation of the total radiation dose without enhanced toxicity.

In conclusion, cisplatin and vinorelbine chemotherapy concurrently combined with standard thoracic radiotherapy and followed by docetaxel consolidation produced promising overall survival in patients with stage III NSCLC, but the vast majority of patients could not continue with the docetaxel consolidation because of toxicity.

ACKNOWLEDGMENTS

REFERENCES

1. Vokes EE, Crawford J, Bogart J, et al. Concurrent chemoradiotherapy for unresectable stage III non-small cell lung cancer. *Clin Cancer Res* 2006;11:5045s–5050s.
2. Auperin A, Le Pechoux C, Pignon JP, et al. Concomitant radio-chemotherapy based on platin compounds in patients with locally advanced non-small cell lung cancer (NSCLC): a meta-analysis of individual data from 1764 patients. *Ann Oncol* 2006;17:473–483.
3. Fournel P, Robinet G, Thomas P, et al. Randomized phase III trial of sequential chemoradiotherapy compared with concurrent chemoradiotherapy in locally advanced non-small-cell lung cancer: Groupe Lyon-Saint-Etienne d'Oncologie Thoracique-Groupeqqfrancaisqqqq de Pneumo-Cancerologie NPC 95-01 Study. *J Clin Oncol* 2006;23:5910–5917.
4. Furuse K, Fukuoka M, Kawahara M, et al. Phase III study of concurrent versus sequential thoracic radiotherapy in combination with mitomycin, vindesine, and cisplatin in unresectable stage III non-small-cell lung cancer. *J Clin Oncol* 1999;17:2692–2699.
5. Curran W, Scott CJ, Langer C, et al. Long-term benefit is observed in a phase III comparison of sequential vs concurrent chemo-radiation for patients with unresected stage III NSCLC: RTOG 9410. *Proc Am Soc Clin Oncol* 2003;22:621 (abstr 2499).
6. Sekine I, Noda K, Oshita F, et al. Phase I study of cisplatin, vinorelbine, and concurrent thoracic radiotherapy for unresectable stage III non-small cell lung cancer. *Cancer Sci* 2004;95:691–695.
7. Fossella FV, DeVore R, Kerr RN, et al. Randomized phase III trial of docetaxel versus vinorelbine or ifosfamide in patients with advanced non-small-cell lung cancer previously treated with platinum-containing chemotherapy regimens. The TAX 320 Non-Small Cell Lung Cancer Study Group. *J Clin Oncol* 2000;18:2354–2362.
8. Shepherd FA, Dancey J, Ramlau R, et al. Prospective randomized trial of docetaxel versus best supportive care in patients with non-small-cell lung cancer previously treated with platinum-based chemotherapy. *J Clin Oncol* 2000;18:2095–2103.
9. Fossella FV, Lee JS, Shin DM, et al. Phase II study of docetaxel for advanced or metastatic platinum-refractory non-small-cell lung cancer. *J Clin Oncol* 1995;13:645–651.
10. Gandara DR, Chansky K, Albain KS, et al. Consolidation docetaxel after concurrent chemoradiotherapy in stage IIIB non-small-cell lung cancer: phase II Southwest Oncology Group Study S9504. *J Clin Oncol* 2003; 21:2004–2010.
11. Therasse P, Arbuck SG, Eisenhauer EA, et al. New guidelines to evaluate the response to treatment in solid tumors. European Organization for Research and Treatment of Cancer, National Cancer Institute of the United States, National Cancer Institute of Canada. *J Natl Cancer Inst* 2000;92: 205–216.
12. Simon R. Optimal two-stage designs for phase II clinical trials. *Control Clin Trials* 1989;10:1–10.
13. Armitage P, Berry G, Matthews J. Survival analysis. In Armitage P, Berry G, Matthews J (eds.), *Statistical Methods in Medical Research* (4th ed.). Oxford: Blackwell Science Ltd, 2002, pp. 568–590.
14. Belani CP, Choy H, Bonomi P, et al. Combined chemoradiotherapy regimens of paclitaxel and carboplatin for locally advanced non-small-cell lung cancer: a randomized phase II locally advanced multi-modality protocol. *J Clin Oncol* 2006;23:5883–5891.
15. Carter D, Keller A, Tolley R, et al. A randomized phase III trial of combined paclitaxel, carboplatin, and radiation therapy followed by either weekly paclitaxel or observation in patients with stage III non-small cell lung cancer. *Proc Am Soc Clin Oncol* 2006;22:635s (abstr 7076).
16. Mac Manus MP, Hicks RJ, Matthews JP, et al. Metabolic (FDG-PET) response after radical radiotherapy/chemoradiotherapy for non-small cell lung cancer correlates with patterns of failure. *Lung Cancer* 2006; 49:95–108.

815

REVIEW ARTICLE

Tatsuo Ohira · Yasuhiro Suga · Yoshitaka Nagatsuka
Jitsuo Usuda · Masahiro Tsuboi · Takashi Hirano
Norihiko Ikeda · Harubumi Kato

Early-stage lung cancer: diagnosis and treatment

Introduction

The lung cancer death rate is increasing throughout the world due to increases in numbers of the elderly, increased environmental pollution, and lack of detection in early stages. At our institution, the 5-year survival rate has gradually improved over the past five decades. These results could be due to improvements in therapeutic procedures, including surgery, chemotherapy, radiotherapy, laser therapy, and immunotherapy. Furthermore, the improvement in survival in Japan may be partially due to mass screening for lung cancer mandated by the Health Insurance Act of 1987. The therapeutic results for lung cancer are unsatisfactory. The 5-year survivals of lung cancer patients according to the Japanese Lung Cancer Registry, are shown in Fig. 1.[1] Good results were obtained only in stage I, but in other stages the results were still disappointing. Thus, in order to reduce deaths from lung cancer, it is necessary to detect and treat early-stage lung cancer.

However, there are various problems in the treatment of early-stage lung cancer. Early-stage lung cancers are classified into two categories according to the location of the tumor: central type and peripheral type, and the treatment of each type has specific problems.

In Japan, the criteria of early-stage lung cancer were first proposed about 30 years ago, in 1975. Peripheral-type early-stage lung cancer was defined as a tumor located in an airway more peripheral than the subsegmental bronchi, with the longest dimension of the tumor being 2 cm or less and with no recognized lymph node or distant metastases. In central-type early-stage lung cancer, the tumor is located in a segmental bronchus. In central-type lesions, even if they are early-stage lung cancer, resection of a large volume of lung is generally necessary. This could be a significant factor for pulmonary dysfunction, especially in older patients. In addition, lung cancer, especially the early-stage central type, has a tendency to develop in multiple lesions. In such cases resection is not a valid option for the treatment of all lesions. Therefore, noninvasive therapeutic modalities were required. Laser therapy has been developed for central-type early lung cancer. For the diagnosis of early-stage central-type lung cancer, autofluorescence fiberscopes, bronchofiberscopic echograms, and optical coherence tomography (OCT) have been developed.

As stated above, the improvement of survival in Japan may be partially due to mass lung cancer screening mandated by the Health Insurance Act of 1987. Mass screening for lung cancer by chest computed tomography (CT) was begun in Japan 10 years ago and is now being used in the United States and Europe. Because large numbers of tiny peripheral lung shadows were detected in many of the CT screening pilot trials,[2,3] it is important to establish an internationally accepted definition of peripheral-type early-stage lung cancer.

Therapeutic guidelines for central-type early-stage lung cancer

In Japan, the therapeutic guidelines for lung cancer were established according to evidence-based medicine, with the support of the Ministry of Health, Labor, and Welfare in 2002. In these guidelines, surgical resection and photodynamic therapy (PDT) are recommended for the treatment of central-type early-stage lung cancer.[4]

T. Ohira (✉) · Y. Suga · Y. Nagatsuka · J. Usuda · M. Tsuboi ·
T. Hirano · H. Kato
Department of Thoracic Surgery, Tokyo Medical University,
6-7-1 Nishi-shinjuku, Shinjuku-ku, Tokyo 160-0023, Japan
Tel. +81-3-3342-6111; Fax +81-3-3342-6154
e-mail: tatsuo@rd5.so_net.ne.jp

N. Ikeda
Department of Thoracic Surgery, International University of Health
and Welfare, Tokyo, Japan